

## Scattering of two particles in a one-dimensional lattice

Seth T. Rittenhouse<sup>1,\*</sup>, P. Giannakeas<sup>2</sup>, and Nirav P. Mehta<sup>3</sup>

<sup>1</sup>*Department of Physics, the United States Naval Academy, Annapolis, Maryland 21402, USA*

<sup>2</sup>*Max-Planck-Institut für Physik komplexer Systeme, Nöthnitzer Street 38, D-01187 Dresden, Germany*

<sup>3</sup>*Department of Physics and Astronomy, Trinity University, San Antonio, Texas 78212, USA*



(Received 14 June 2021; accepted 16 July 2021; published 6 August 2021)

This study concerns the two-body scattering of particles in a one-dimensional periodic potential. A convenient ansatz allows for the separation of center-of-mass and relative motion, leading to a discrete Schrödinger equation in the relative motion that resembles a tight-binding model. A lattice Green's function is used to develop the Lippmann-Schwinger equation, and ultimately derive a multiband scattering  $K$  matrix which is described in detail in the two-band approximation. Two distinct scattering lengths are defined according to the limits of zero relative quasimomentum at the top and bottom edges of the two-body collision band. Scattering resonances occur in the collision band when the energy is coincident with a bound state attached to another higher or lower band. Notably, repulsive on-site interactions in an energetically closed lower band lead to collision resonances in an excited band.

DOI: [10.1103/PhysRevA.104.023308](https://doi.org/10.1103/PhysRevA.104.023308)

### I. INTRODUCTION

Ultracold gases embedded in optical lattices present numerous theoretical and experimental opportunities for the investigation of few- and many-body physics [1,2]. Such systems provide a versatile platform for a number of reasons. Control of the laser intensity, wavelength, and beam geometry enable detailed tunability of the depth, spacing, and geometry of the lattice. Moreover, the variety of atomic species that have been successfully trapped includes Bose, Fermi, and even mixed-symmetry systems [2–4], all of which can be studied by tuning their mutual interactions via Feshbach resonances [5]. For example, bosonic ensembles in a lattice permitted the realization of a many-body phase transition from superfluid to Mott insulator [6,7], and site-resolved imaging of Bose [8,9] and Fermi [10,11] systems has enabled yet more flexibility.

In addition, two-dimensional (2D) Fermi gases in lattices are proposed as candidates to study topological many-body phases such as  $p$ -wave superfluidity [12]. Recently, ultracold atoms in driven optical lattices proved to be a panacea for the experimental realization of time crystals [13–15]; an exotic many-body phase that features a broken translation symmetry both in space and time, where Wilczek's [16] initial proposal laid the ground for a more systematic theoretical understanding [17–20]. Furthermore, nonequilibrium dynamics in one-dimensional (1D) lattices induced via interaction quenches on few-bosonic ensembles result in the formation of global density waves [21,22], directional transport by spatially modulated interactions [23], and many-body expansion in weakly interacting Bose-Fermi mixtures [24].

Apart from these advances in the realm of many-body physics, studies on the few-body aspects of ultracold atoms in lattice geometries explore their multifaceted collisional properties, such as the formation of bound pairs [25–30], lattice-induced resonances [31–33], Feshbach resonances in lattices [34], and the physics of reactive and Umklapp processes [35]. More refined theoretical studies on the two-body collisional physics permitted the inclusion of finite range effects [36] and explored the impact of the energetically higher bands [35,37]. Two-body collisions on a lattice occur within a set of energy bands which loosely behave as collision channels, with two-body interactions yielding intra and interband effects on collisional processes [37] similar to the behavior seen in confinement-induced resonances [38]. Beyond the two-body physics, theoretical studies have shown the existence of three-body bound states in both three-dimensional (3D) and 1D lattices [39,40]. Additionally, in such systems an on-site attractive three-body interaction can emerge that induces an instability yielding thus the collapse of the many-body ground state [41]. Evidently, the detailed understanding of scattering processes in lattice geometries, and the necessary conditions under which resonant phenomena can occur, is of paramount importance to the design and manipulation of exotic many-body phases.

In this work a systematic pathway to address collisional physics of two particles, with either bosonic or fermionic character, in the presence of a periodic potential is developed based on the  $K$ -matrix formalism. Within this formalism, the energy-normalized Bloch states are employed as scattering waves incorporating contributions from both energetically accessible (open) and inaccessible (closed) bands. In agreement with previous works, we observe that for attractive interactions comparable in strength to the band gap, a resonance arises for scattering between particles in the lowest band due to virtual transitions into the closed bands

\*Corresponding author: [rittenho@usna.edu](mailto:rittenho@usna.edu)

[27,32,33,36,37,42]. Furthermore, we observe that for repulsive on-site interactions with energy similar to the band gap additional resonant features occur for scattering of two particles in an *excited* band.

The paper is organized as follows. In Sec. II, we describe the two-body, multiband Hamiltonian in a basis of Wannier states and separate it into discrete center-of-mass and relative motion coordinates. In Sec. III we develop the Green's operator for the relative noninteracting Hamiltonian via a lattice Green's function for both energetically open and closed bands. In Sec. IV we derive the lattice  $K$  matrix for two-body, on-site interactions, and examine the special case where each particle can occupy only two energy bands. In Sec. V we derive the lattice scattering length, which can be used to describe the interaction between two particles at energies near the top or bottom of the two-body bands. Finally, in Sec. VI we summarize our results and discuss future work.

## II. ONE-DIMENSIONAL LATTICE

In this section, we describe a system consisting of two particles confined to a periodic 1D potential  $V_{\text{lat}}(x)$  with periodicity  $\lambda$ . In the absence of a two-body interaction the behavior of each particle is described by the simple Hamiltonian  $\widehat{\mathcal{H}}_0 = -\frac{\hbar^2}{2m} \frac{d^2}{dx^2} + V_{\text{lat}}(x)$  which is diagonalized by a Bloch function  $\phi_\mu(q; x)$  where  $\mu$  is a band index and  $q$  is the quasimomentum. Bloch waves are delocalized functions that extend throughout the entire lattice. However, they can be combined into an orthonormal basis localized to each lattice site for each band. These are the Wannier functions which take the form

$$w_{\mu n}(x) = \left( \frac{\lambda}{2\pi} \right)^{1/2} \int_{-\pi/\lambda}^{\pi/\lambda} e^{iqn\lambda} \phi_\mu(q; x) dq. \quad (1)$$

Here, beyond the band index  $\mu$ , there is an additional index in the Wannier functions; the site index  $n \in \mathbb{Z}$  specifying the lattice site location  $x = n\lambda$  at which the function is localized.

The behavior of a single particle in the lattice is characterized by the Hamiltonian

$$\begin{aligned} \hat{h} = & \sum_{\mu, n} \epsilon_\mu |\mu n\rangle \langle \mu n| \\ & - \sum_{\mu, n, j > 0} S_j^\mu (|\mu n\rangle \langle \mu(n+j)| + |\mu(n+j)\rangle \langle \mu n|), \end{aligned} \quad (2)$$

where  $|\mu n\rangle$  is the Wannier state associated with a particle in the  $\mu$ th band localized to the  $n$ th lattice site. Here,  $\epsilon_\mu = \langle \mu n | \widehat{\mathcal{H}}_0 | \mu n \rangle$  is the on-site energy and  $S_j^\mu = -\langle \mu n | \widehat{\mathcal{H}}_0 | \mu(n+j) \rangle$  is the energy associated with the particle hopping  $j$  sites from site  $n$  to site  $n \pm j$ . Note that we assumed that the band energies are symmetric in the quasimomentum  $q$ . Diagonalizing this Hamiltonian gives, not at all surprisingly, the band dispersion relation written as its cosine Fourier transform, i.e.,

$$E_\mu(q) = \epsilon_\mu - \sum_{j=1}^{\infty} 2S_j^\mu \cos(jq). \quad (3)$$

In this work we will focus on the deep lattice regime in which Wannier states are localized to a single lattice site and tunneling to more distant sites is suppressed. This results in a strong

suppression in the hopping energy  $S_j^\mu$  for  $j > 1$ . Thus, for the purposes of this work, we will assume only nearest-neighbor hopping terms survive, i.e.,  $S_j^\mu = S_\mu \delta_{1,j}$ .

With the single-particle discrete Hamiltonian in hand, we may now proceed to write the two-body Hamiltonian in terms of the localized discrete Wannier basis. In first quantized form, the full Hamiltonian is given by

$$\hat{H} = \hat{h}_1 + \hat{h}_2 + \hat{V}, \quad (4)$$

where  $\hat{h}_j$  is the single-particle Hamiltonian Eq. (2) for particle  $j$ , and  $\hat{V}$  is the interaction between the two particles. In the Wannier basis, the interaction is expressed as

$$\hat{V} = \sum_{\substack{\mu, \nu, \mu', \nu' \\ m, n}} U_{\mu', \nu'}^{\mu, \nu} (|n-m\rangle | \mu m; \nu n \rangle \langle \mu' m; \nu' n |). \quad (5)$$

Here,  $|\mu m; \nu n\rangle$  represents the two-body Wannier state of particle 1 in band  $\mu$  localized to site  $m$  and particle 2 in band  $\nu$  localized to site  $n$ . This interaction matrix element is given by

$$U_{\mu', \nu'}^{\mu, \nu} (|n-m\rangle) = \langle \mu m; \nu n | V_{\text{int}}(x_1 - x_2) | \mu' m; \nu' n \rangle,$$

where  $V_{\text{int}}(x)$  is the 1D interaction potential. In this work we will be concerned with short-range interactions with Wannier states localized to a single lattice site leading to on-site interactions  $U_{\mu', \nu'}^{\mu, \nu} (|n-m\rangle) = U_{\mu', \nu'}^{\mu, \nu} \delta_{m,n}$ . We leave the interaction in a more general form here for completeness, and it will be specified in Sec. IV A. We note here that for there to be nearest-neighbor hopping, there must be a nonzero probability amplitude of the Wannier state in the neighboring lattice site. This might lead one to think that there also must be a nearest-neighbor interaction, i.e.,  $U_{\mu', \nu'}^{\mu, \nu} (|n-m\rangle) \neq 0$ . However, for interaction potentials with a range much smaller than the lattice spacing, the nearest-neighbor interaction matrix element is determined by the total probability of tunneling to a neighboring site. Therefore, in the limit of small hopping energy, nearest-neighbor interactions are exponentially suppressed and are ignored in this work.

The eigenfunctions of  $\hat{H}$  can be expanded in the Wannier basis as  $|\Psi\rangle = \sum_{\mu \nu m n} \Psi_{\mu, \nu}^{m, n} |\mu m; \nu n\rangle$ , leading to the discrete Schrödinger equation

$$\begin{aligned} (E - \epsilon_\mu - \epsilon_\nu) \Psi_{\mu, \nu}^{m, n} = & -S_\mu [\Psi_{\mu, \nu}^{(m+1), n} + \Psi_{\mu, \nu}^{(m-1), n}] \\ & -S_\nu [\Psi_{\mu, \nu}^{m, (n+1)} + \Psi_{\mu, \nu}^{m, (n-1)}] \\ & + \sum_{\mu', \nu'} U_{\mu', \nu'}^{\mu, \nu} (|n-m\rangle) \Psi_{\mu', \nu'}^{m, n}. \end{aligned} \quad (6)$$

### Center-of-mass separation

The most important aspect of the discrete Schrödinger equation in Eq. (6) is that it can be separated into the discrete center-of-mass  $Z = (m+n)/2$  and relative separation  $z = m-n$  coordinates with the separation ansatz

$$\Psi_{\mu, \nu}^{(Z+z/2), (Z-z/2)} \propto \psi_{\mu, \nu}(z) e^{iK\lambda Z + i\phi_K^{\mu\nu} z}, \quad (7)$$

where  $K$  is the center-of-mass quasimomentum. Here the angle

$$\phi_K^{\mu\nu} = \arg(S_\mu e^{iK\lambda/2} + S_\nu e^{-iK\lambda/2}), \quad (8)$$

is included to subtract a constant offset in the relative motion quasimomentum. Inserting this ansatz into Eq. (6) yields the discrete Schrödinger equation in the separation coordinate

$$E\psi_{\mu\nu}(z) = \varepsilon_{\mu\nu}\psi_{\mu\nu}(z) - [J_K^{\mu\nu}\psi_{\mu\nu}(z+1) + J_K^{\mu\nu}\psi_{\mu\nu}(z-1)] + \sum_{\mu'\nu'} e^{i(\phi_k^{\mu'\nu'} - \phi_k^{\mu\nu})z} U_{\mu',\nu'}^{\mu,\nu}(|z|)\psi_{\mu'\nu'}(z), \quad (9)$$

where the relative-coordinate hopping and two-body on-site energy are defined as

$$J_K^{\mu\nu} = \sqrt{S_\mu^2 + S_\nu^2 + 2S_\mu S_\nu \cos(K\lambda)},$$

$$\varepsilon_{\mu\nu} = \varepsilon_\mu + \varepsilon_\nu.$$

Note that the separated Schrödinger equation is now in the form of a simple tight-binding model with nearest-neighbor hopping with “on-site energies” that are modified by the interaction matrix elements  $U_{\mu',\nu'}^{\mu,\nu}(|z|)$ . Also note that in the relative coordinate  $z$ , the hopping energies  $J_K^{\mu\nu}$  are now dependent on the center-of-mass quasimomentum  $K$ .

In the absence of interactions, Eq. (9) is solved simply by plane waves in the relative coordinates, i.e.,

$$\psi_{\mu\nu}(z) \propto e^{ik\lambda z},$$

where  $k$  is the relative coordinate quasimomentum. The resulting dispersion relations define two-body energy bands that depend on the center-of-mass motion with dispersion

$$\varepsilon_{\mu\nu}(K, k) = \varepsilon_{\mu\nu} - 2J_K^{\mu\nu} \cos \lambda k. \quad (10)$$

### III. LATTICE GREEN'S FUNCTION

To examine scattering of two particles in the lattice described above, we must first construct the Green's operator associated with the relative coordinate Hamiltonian at fixed center-of-mass quasimomentum  $K$  given by

$$\hat{H}_{\text{rel}} = \hat{h}_{\text{rel}} + \hat{U},$$

$$\hat{h}_{\text{rel}} = \sum_{\mu,\nu,z} \varepsilon_{\mu\nu} |K; \mu\nu z\rangle \langle K; \mu\nu z| - \sum_{\mu,\nu,z} J_K^{\mu\nu} (|K; \mu\nu(z+1)\rangle \langle K; \mu\nu z| + |K; \mu\nu(z-1)\rangle \langle K; \mu\nu z|),$$

$$\hat{U} = \sum_{\substack{\mu,\nu \\ \mu',\nu' \\ z}} e^{i(\phi_k^{\mu'\nu'} - \phi_k^{\mu\nu})z} U_{\mu',\nu'}^{\mu,\nu}(|z|) |K; \mu\nu z\rangle \langle K; \mu'\nu' z|, \quad (11)$$

where  $\hat{h}_{\text{rel}}$  is the noninteracting relative Hamiltonian and  $\hat{U}$  is the interaction. Here, we define the basis state  $|K; \mu\nu z\rangle$  as the state where the two particles have a center-of-mass motion defined by quasimomentum  $K$  and a particle separation of  $z$  with particle 1 in band  $\mu$  and particle 2 in band  $\nu$ , i.e.,

$$|K; \mu\nu z\rangle = \mathcal{N} \sum_{Z=0}^N e^{iK\lambda Z} |\mu(Z+z/2); \nu(Z-z/2)\rangle,$$

where  $\mathcal{N}$  is a normalization constant.

We will define the lattice Green's operator  $\hat{G}$  such that

$$\langle K; \mu'\nu' z' | (\hat{h}_{\text{rel}} - E) \hat{G} | K; \mu\nu z \rangle = \delta_{\mu\mu'} \delta_{\nu\nu'} \delta_{zz'}.$$

We will proceed to find  $\hat{G}$  by expanding it in the Wannier states, i.e.,

$$\hat{G} = \sum_{\substack{\mu\nu \\ z', z}} g_{\mu\nu}(K; z, z') |K; \mu\nu z\rangle \langle K; \mu\nu z'|, \quad (12)$$

where  $g_{\mu\nu}(K; z, z')$  is the lattice Green's function (LGF) which is a solution to

$$\delta_{z,z'} = (\varepsilon_{\mu\nu} - E)g_{\mu\nu}(K; z, z') - J_K^{\mu\nu} [g_{\mu\nu}(K; z+1, z') + g_{\mu\nu}(K; z-1, z')]. \quad (13)$$

For the purposes of this work, we are concerned with even parity states associated with two bosons or two spin-1/2 fermions in a singlet state. Therefore, below we will only consider even parity solutions to Eq. (13)

The even parity LGF can be broken into two cases: (1) When the scattering energy  $E$  is within the available two-body energies  $\varepsilon_{\mu\nu}(K, k)$  corresponding to an open two-body scattering band; or (2) when  $E$  lies outside of the available energies defined by  $\varepsilon_{\mu\nu}(K, k)$  corresponding to a closed two-body scattering band.

#### A. Open-band Green's function

For energies within the  $\{\mu, \nu\}$  two-body band (i.e.,  $|E - \varepsilon_{\mu\nu}| < 2|J_K^{\mu\nu}|$ ), we can define the relative quasimomentum  $k$  through the dispersion relation in Eq. (10). For  $z \neq z'$  Eq. (13) are solved by the ansatz

$$g_{\mu\nu}(K; z, z') = A \sin(k\lambda z_{>}) \cos(k\lambda z_{<}),$$

where  $z_{>(<)}$  is the larger (smaller) of  $z$  and  $z'$ . Here we chose to use the principle value Green's function which obeys standing-wave boundary conditions. This is similar to the approach taken in other works [37,38,43] in which the singular portion of the Green's function corresponding to direct classical trajectories is separated and removed. The remaining constant  $A$  can be found by simply inserting the ansatz into Eq. (13) for  $z = z'$  giving

$$g_{\mu\nu}(K; z, z') = -\frac{\sin(k\lambda z_{>}) \cos(k\lambda z_{<})}{J_K^{\mu\nu} \sin(k\lambda)}. \quad (14)$$

This can be further simplified by writing it in terms of the regular  $f_{\mu\nu}^+$  and irregular  $f_{\mu\nu}^-$  band-energy normalized scattering solutions of the noninteracting Hamiltonian given, respectively, by

$$f_{\mu\nu}^+(z) = \sqrt{\frac{\lambda}{\pi |v_g^{\mu\nu}|}} \cos(k\lambda z),$$

$$f_{\mu\nu}^-(z) = \sqrt{\frac{\lambda}{\pi |v_g^{\mu\nu}|}} \sin(k\lambda z), \quad (15)$$

$$v_g^{\mu\nu} = 2\lambda J_K^{\mu\nu} \sin(\lambda k) = \frac{\partial \varepsilon_{\mu\nu}(K, k)}{\partial k},$$

so that  $\sum_z f_{\mu\nu}^{\pm*}(E; z) f_{\mu\nu}^{\pm}(E'; z) = \delta(E - E')$ . In terms of  $f_{\mu\nu}^+$  and  $f_{\mu\nu}^-$  the open-band LGF is now given by

$$g_{\mu\nu}(K; z, z') = -2\pi f_{\mu\nu}^+(z_{<}) f_{\mu\nu}^-(z_{>}). \quad (16)$$

### B. Closed-band Green's function

For energies outside of the  $\{\mu, \nu\}$  two-body energy band (when  $|E - \varepsilon_{\mu\nu}| > 2|J_K^{\mu\nu}|$ ) we have a slightly different situation, where the probability of the two particles has to vanish at large separation distances, i.e.,  $|z - z'| \rightarrow \infty$ . This implies that in this limit the LGF must obey exponentially decaying boundary conditions. Namely, for this case the  $z \neq 0$  is solved by the ansatz [36]

$$g_{\mu\nu}(K; z, z') = A\alpha^{|z-z'|},$$

where  $\alpha$  is defined as the solution to

$$E - \varepsilon_{\mu\nu} = -J_K^{\mu\nu} \frac{1 + \alpha^2}{\alpha}, \quad (17)$$

where we restrict  $|\alpha| \leq 1$ . Again the coefficient  $A$  can be found by inserting the ansatz into Eq. (13) at  $z = z'$ , giving

$$g_{\mu\nu}(K; z, z') = \frac{\alpha^{|z-z'|+1}}{J_K^{\mu\nu}(1 - \alpha^2)}. \quad (18)$$

Note that when  $E < \varepsilon_{\mu\nu} - 2J_K^{\mu\nu}$  (i.e., below the band) Eq. (17) gives  $0 < \alpha < 1$  such that the LGF decays exponentially. When  $E > \varepsilon_{\mu\nu} + 2J_K^{\mu\nu}$  (i.e., above the band) Eq. (17) gives  $-1 < \alpha < 0$  so that the amplitude of the LGF still decays exponentially but with alternating sign.

## IV. SCATTERING FOR ON-SITE INTERACTIONS

Here we will use the Green's operator found above to extract scattering properties of two particles in a 1D lattice interacting via on-site interactions only. The full Schrödinger equation for the relative motion can be solved via the Lippmann-Schwinger equation (LSE) given by

$$|\psi\rangle = |\psi_0\rangle - \hat{G}\hat{U}|\psi\rangle, \quad (19)$$

where the homogeneous solution  $|\psi_0\rangle = \sum_z f_{\mu\nu}^+(z)|K; \mu\nu z\rangle$  is the initial state of the system. Note here that we are using the band-energy normalized scattering states from Eq. (15). In the  $z \rightarrow \infty$  limit, inserting the LGF from Eq. (16) gives the scattering solution

$$\begin{aligned} \psi_{\mu\nu}(z) &= f_{\mu\nu}^+(z) + 2\pi f_{\mu\nu}^-(z) \langle f_{\mu\nu}^+ | \hat{U} | \psi \rangle, \\ \langle f_{\mu\nu}^+ | \hat{U} | \psi \rangle &= \sum_{\mu' \nu' z'} f_{\mu\nu}^+(z') e^{i(\phi_K^{\mu'} - \phi_K^{\mu\nu})z'} \\ &\quad \times U_{\mu', \nu'}^{\mu\nu}(|z'|) \psi_{\mu' \nu'}(z'). \end{aligned} \quad (20)$$

Here we assume the interaction between the two particles is short range in comparison with the lattice's periodicity, i.e.,  $\ell_{\text{int}} \ll \lambda$  where  $\ell_{\text{int}}$  is the lengthscale of the interparticle interaction. Additionally, we assume that the Wannier states are localized to single lattice sites. These two assumptions, sufficiently, imply that the particles interact via on-site interactions only,  $U_{\mu' \nu'}^{\mu\nu}(|z|) = U_{ij} \delta_{z,0}$ , where the double band index  $\{\mu, \nu\}$  is collectively denoted by a single index vector,

i.e.,  $\mathbf{i} = \{\mu, \nu\}$ ,  $\mathbf{j} = \{\mu', \nu'\}$ , and the on-site interaction matrix elements are given by  $U_{ij} = U_{\mu' \nu'}^{\mu\nu}$ .

In addition, Eq. (20) can be generalized to include transitions between two open bands with overlapping energies. From this the lattice  $K$ -matrix element  $\mathbf{K}_{ji}^L$  is identified, which in turn determines the admixture of the irregular solution  $f_j^{(-)}(z)$  in the final band  $\mathbf{j}$ :

$$\begin{aligned} \langle K; \mathbf{j} z | \psi \rangle &= \delta_{ji} f_i^+(z) - \mathbf{K}_{ji}^L f_j^-(z), \\ \mathbf{K}_{ji}^L &= -2\pi \langle f_j^+ | \hat{U} | \psi \rangle, \end{aligned} \quad (21)$$

where  $|f_j^+\rangle = \sum_z f_j^+(z)|K; \mathbf{j} z\rangle$ . Solving this equation self-consistently for the  $K$  matrix yields

$$\mathbf{K}_{ji}^L = -2\pi \langle f_j^+ | (\mathbb{1} + \hat{U}\hat{G})^{-1} \hat{U} | f_i^+ \rangle, \quad (22)$$

where  $\hat{G}$  and  $\hat{U}$  indicate the LGF and interaction operators, respectively.

In the case of on-site interactions  $\hat{U} = \sum_{ij} U_{ij} |K; \mathbf{i} 0\rangle \langle K; \mathbf{j} 0|$ , we show in the Appendix that by partitioning  $\hat{G}$  and  $\hat{U}$  into  $N$  open and  $M$  closed-band contributions the lattice  $K$  matrix for scattering from one open band to another is given by

$$\mathbf{K}^L = -2\lambda \bar{v}_g^{-1/2} [\mathcal{U}_{oo} - \mathcal{U}_{oc} \bar{g}_c (\mathbb{1} + \mathcal{U}_{cc} \bar{g}_c)^{-1} \mathcal{U}_{co}] \bar{v}_g^{-1/2}. \quad (23)$$

Here  $\mathcal{U}_{oo}$  is the  $N \times N$  matrix of interaction matrix elements  $U_{ij}$  for initially and finally open bands.  $\mathcal{U}_{co} = [\mathcal{U}_{oc}]^\dagger$  is the  $M \times N$  matrix of interaction matrix element between the finally closed and initially open bands.  $\mathcal{U}_{cc}$  is the  $M \times M$  matrix of interaction matrix elements for initially and finally closed bands. The  $M \times M$  diagonal matrix  $\bar{g}_c$  has a diagonal of closed channel LGFs evaluated at  $z = z' = 0$ . Finally,  $[\bar{v}_g]^{-1/2}$  is an  $N \times N$  diagonal matrix with diagonal values given by the inverse of the square root of the open-band group velocities  $(v_g^i(k_i))^{-1/2}$ .

The form of Eq. (23) is scattering theory, being quite reminiscent of the standard channel closing formulas of multichannel quantum defect theory [44]. The first term describes the background scattering in the open bands. The second term incorporates the contributions from virtual scattering into energetically closed two-body bands. Notice that including these closed-band terms allows for resonances when  $\det(\mathbb{1} + \mathcal{U}_{cc} \bar{g}_c) = 0$  in the open-band  $K$  matrix  $\mathbf{K}^L$ . In essence, this means that all these virtual transitions in closed bands can collectively give rise to lattice induced resonances in the open bands. Also note that the  $K$  matrix can related to the standard  $S$  matrix via the expression  $\mathbf{S}^L = (\mathbb{1} + i\mathbf{K}^L)(\mathbb{1} - i\mathbf{K}^L)^{-1}$ .

In the absence of other bands, Eq. (23) gives that the  $K$  matrix for single band scattering with on-site interactions is simply proportional to the interaction strength as expected. By analogy to this, in a single open band, the contributions from excited bands results in a quasimomentum-dependent effective interaction given by

$$U_{\text{eff}} = \mathcal{U}_{oo} - \mathcal{U}_{oc} \bar{g}_c (\mathbb{1} + \mathcal{U}_{cc} \bar{g}_c)^{-1} \mathcal{U}_{co}. \quad (24)$$

Properly including these effects in many-body models like the Bose-Hubbard model is likely quite important, especially in the presence of the above-mentioned lattice-induced resonances.



We note that in Ref. [32], the resonance structure seen in Eqs. (23) and (24) was described through an effective two-body, two-state Hamiltonian where the corresponding parameters are fitted directly from numerical calculations. In the present work we derive these results directly, illustrating how the virtual transitions to closed bands lead to resonant processes.

### A. Two-band approximation

Here we simplify our system by assuming a simple two-band approximation. We will assume that each particle is in the Wannier states  $w_\mu(x)$  corresponding to either the lowest band ( $\mu = 0$ ) or the first excited band ( $\mu = 1$ ) meaning that the available two-body states are restricted to  $\{\mu, \nu\} = \{0, 0\}, \{0, 1\}, \{1, 0\},$  and  $\{1, 1\}$ . If we assume that the interaction potential is symmetric under inversion and the Wannier states are parity eigenstates, then the two-body state with one particle in the excited band is decoupled by parity, i.e.,  $U_{00}^{10} = U_{11}^{10} = 0$ . We will further assume that the interaction potential  $V(x)$  is short-range enough to be approximated by a contact interaction. For notational simplicity we will label the interaction matrix elements  $U_{\mu\nu}^{\mu'\nu'}$  as  $U_{00}^{00} = U_{00}, U_{01} = U_{10} = U_{00}^{11} = U_{11}^{00}$ , and  $U_{11} = U_{11}^{11}$ .

If both particles start in the lowest  $\{0, 0\}$  band such that the  $\{1, 1\}$  band is energetically inaccessible, Eq. (23) becomes

$$\mathbf{K}_{00 \rightarrow 00}^L = \frac{-1}{J_K^{00} \sin \lambda k} \times \left[ U_{00} - \frac{U_{01}^2}{U_{11} + \sqrt{(E - \varepsilon_{11})^2 - (2J_K^{11})^2}} \right]. \quad (25)$$

In the case where the on-site interactions in the excited band are attractive, i.e.,  $U_{11} < 0$ , a resonance occurs at precisely the energy of a dimer bound state attached to the *excited* band,  $E_{\text{dim}} = \varepsilon_{11} - \sqrt{U_{11}^2 + (2J_K^{11})^2}$ . Thus, we see that a lattice-induced resonance occurs due to virtual scattering into a bound state attached to an excited band that energetically lies in the continuum of the lower band. Intuitively, this means that the lattice-induced resonances fulfill a Fano-Feshbach-like scenario where the continuum is structured into bands due to the presence of the lattice. Furthermore, by setting the the interband coupling elements to zero, i.e.,  $U_{01} = 0$  in Eq. (25), the single-band lattice scattering behavior is recovered.

Unlike scattering in free space, the energy bands induced by the lattice allow the existence of scattering channels at energies *below* the scattering energy that are energetically inaccessible. In the case of the two-band approximation this means that two particles scattering in the excited band can go through virtual scattering processes in a lower, energetically inaccessible band. The  $K$  matrix for the  $\{1, 1\} \rightarrow \{1, 1\}$  scattering process is given from Eq. (23) as

$$\mathbf{K}_{11 \rightarrow 11}^L = \frac{-1}{J_K^{11} \sin \lambda k} \times \left[ U_{11} - \frac{U_{01}^2}{U_{00} - \sqrt{(E - \varepsilon_{00})^2 - (2J_K^{00})^2}} \right]. \quad (26)$$

In this case we can see that a scattering resonance occurs for  $U_{00} > 0$  when a state is bound *above* the lowest band at energy  $E_{\text{dim}} = \varepsilon_{00} + \sqrt{U_{00}^2 + (2J_K^{00})^2}$  is embedded in the excited two-body band. Counterintuitively, this brings about the possibility for *repulsive* on-site interactions in an energetically closed lower band inducing *resonant* interactions in an excited band. This might be relevant for the case of spin-1/2 fermions in which the Fermi level is at the bottom of an excited band. In this case, it might be possible for repulsive on-site interactions between opposite spin particles in the lowest band to induce strong effectively attractive interactions in particles at the Fermi level in the conduction band.

Figure 1 shows the  $K$  matrix for scattering in the lowest and first excited two-body bands assuming that the lattice potential is deep enough that the lowest several Wannier states can be approximated by oscillator states, i.e.,  $w_\mu(x) \propto e^{-x^2/2\ell_{\text{HO}}^2} H_n(\frac{x}{\ell_{\text{HO}}})$ , where  $\ell_{\text{HO}}$  is the local oscillator length near the bottom of a lattice site and  $H_n(y)$  is a Hermite polynomial. Here, the interaction potential is taken to be a simple contact interaction whose strength is governed by the 1D free-space scattering length

$$V_{\text{int}}(x_1 - x_2) = -\frac{2\hbar^2}{ma_{1\text{D}}} \delta(x_1 - x_2).$$

Experimentally, in the presence of a strong transverse confinement,  $a_{1\text{D}}$  could be tuned using a confinement-induced resonance [38]. With these assumptions we can calculate all of the relevant parameters from Eqs. (2) and (4). The resulting  $K$ -matrix element for scattering in the lowest band  $\mathbf{K}_{00 \rightarrow 00}^L$  is shown as a color density plot in Fig. 1(a). The  $K$ -matrix element is plotted as a function of  $K$  (in units of  $1/\lambda$ ) on the horizontal axis, and  $E$  (shifted to the center of the  $\{0,0\}$  band and in units of  $|S_0|$ ) on the vertical axis. The local oscillator length is set so that  $\ell_{\text{HO}} = \lambda/8$ . The lattice-free 1D scattering length  $a_{1\text{D}}$  has been set by requiring the binding energy of a bound state attached to the excited band to intersect the upper part of the  $\{0,0\}$  two-body band at center-of-mass quasimomentum  $\lambda K = 3\pi/4$ . Also shown is the energy of the bound state attached to the excited two-body band, indicated by the red dashed line. Here we can clearly see the resonance that occurs when the bound state is at energies accessible in the band. Figure 1(b) shows the  $K$  matrix for scattering in the excited band  $\mathbf{K}_{11 \rightarrow 11}^L$  for the same lattice parameters with a 1D lattice-free scattering length set to be negative with a bound state attached to the *lower* band intersecting the lower portion of the  $\{1,1\}$  two-body band at  $\lambda K = 3\pi/4$ . Note that in both Figs. 1(a) and 1(b), we multiplied the  $K$  matrix by  $J_K^{\mu\nu} \sin(\lambda k)$  to remove the singularities at the edge of the two-body band (when  $\lambda k = 0, \pm\pi$ ). The energy of the bound state attached to the lower two-body band is shown as a dashed red line in Fig. 1(b). As the state cuts through the band, the related a scattering resonance can be seen in  $\mathbf{K}_{11 \rightarrow 11}^L$ .

### B. Beyond two-band approximation

In the case of scattering in the lowest two-body band in the presence of more than one excited band, if the excited bands are uncoupled, the above results can be easily extended

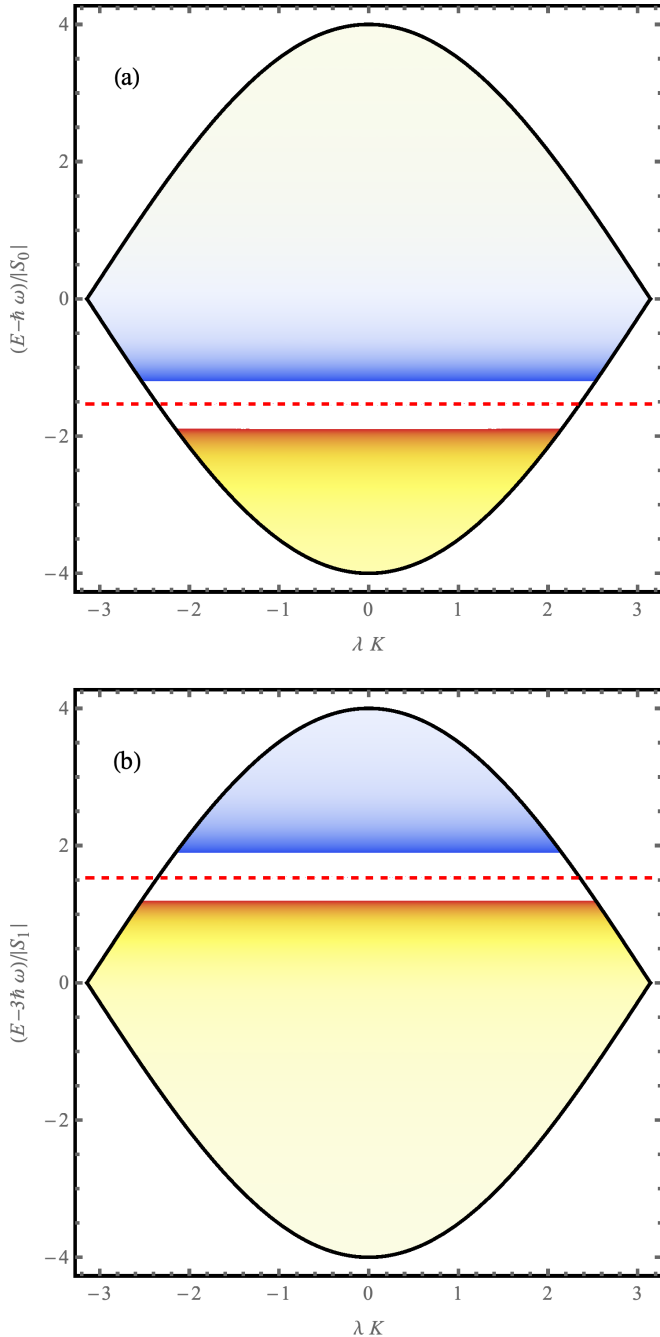


FIG. 1. A color density plot of the elastic scattering  $K$ -matrix element  $J_K^{\mu\nu} \sin(k\lambda) \mathbf{K}_{\mu\nu \rightarrow \mu\nu}^L$  under the two-band approximation with harmonic oscillator Wannier states is shown for (a) scattering in the lowest two-body band  $\{0, 0\} \rightarrow \{0, 0\}$  with  $\lambda = 8\ell_{HO}$  and  $a_{1D}$  set so that the excited-band bound state intersects the lower two-body band at  $\lambda K = 3\pi/4$ . The same is shown in (b) for scattering in the first excited band  $\{1, 1\} \rightarrow \{1, 1\}$  with  $\lambda = 8\ell_{HO}$  and  $a_{1D}$  set so that the bound state attached to the lower band intersects the lower portion of the two-body band at  $\lambda K = 3\pi/4$ . The lower yellow region and upper blue regions represent positive and negative values of the  $K$ -matrix element, respectively, with the darker color indicating a larger magnitude. In both (a) and (b) the solid black curves mark the edge of the respective two-body bands while the dashed red curves represent the position of a bound state attached to the (a) excited and (b) ground two-body bands.

to give

$$\mathbf{K}_{00 \rightarrow 00}^L = -\frac{1}{J_K^{00} \sin \lambda k} \left[ U_{00}^{00} - \sum_{\{\mu\nu\} \neq \{00\}} \frac{|U_{\mu\nu}^{00}|^2}{U_{\mu\nu}^{\mu\nu} + \sqrt{(E - \varepsilon_{\mu\nu})^2 - (2J_K^{\mu\nu})^2}} \right].$$

The sum here accounts for virtual scattering into each excited band. Notice that a properly tuned attractive interaction diagonal matrix element in an excited band  $U_{\mu\nu}^{\mu\nu}$  can create a bound state attached to that two-body band that cuts through the lowest band creating a scattering resonance, similarly to Fig. 1(a). Coupling between excited bands can shift the position of these bound states. However, even with these shifts, if the states become degenerate with the  $\{\mu\nu\} = \{00\}$  band, we expect a band-induced scattering resonances to occur.

In the case of scattering in excited bands, it is possible for multiple excited two-body bands to overlap in energy. In this case, whenever the scattering energy and center-of-mass quasimomentum place the system in the overlap region of multiple two-body bands Eq. (23) still holds, but the  $K$  matrix is an  $N \times N$  matrix where  $N$  is the number of overlapping bands. The diagonal elements of  $\mathbf{K}^L$  represent elastic scattering processes where the incident and outgoing states are in the same bands. However, the off-diagonal elements indicate inelastic scattering processes where the energy and center-of-mass quasimomentum  $K$  of the system is conserved, but the relative quasimomentum  $k$  is not.

For example, in the case where the lattice sites are deep enough to be treated locally as harmonic oscillators, the  $\{\mu\nu\} = \{11\}$  band overlaps with the  $\{20\}$  and  $\{02\}$  bands meaning that the lattice  $K$  matrix,  $\mathbf{K}^L$ , is a  $3 \times 3$  matrix (or  $2 \times 2$  in the case of symmetrized states for bosonic scattering). The  $K$ -matrix elements are shown in Figs. 2(a) to 2(d) for the case of the  $\{1, 1\}$  and the symmetrized  $\{0, 2\}$  two-body bands overlapping. Here, the lattice and interaction parameters are set to be the same as in Fig. 1(b). The solid and dotted black lines show the edges of the  $\{1, 1\}$  and the symmetrized  $\{0, 2\}$  two-body bands, respectively. The position of a resonant state attached to the lower  $\{0, 0\}$  band is shown as the red dashed curve. The  $\{0, 2\}$  band completely encloses the  $\{1, 1\}$  band. Figures 2(b) and 2(c), showing the  $\mathbf{K}_{11 \rightarrow 02}^L$  and  $\mathbf{K}_{02 \rightarrow 11}^L$  inelastic  $K$ -matrix element, respectively, are identical. According to Eq. (23) the  $\mathbf{K}_{11 \rightarrow 11}^L$  matrix element is the same as in the two-band case given in Eq. (26) and thus Fig. 2(a) is the same as Fig. 1(b) but plotted on a different energy scale. Notice that a resonance appears at the same energy for all  $K$ -matrix elements.

Notice in Eq. (23) that the resonance condition  $\det(\mathbb{1} + \mathcal{U}_{cc} \bar{g}_c) = 0$  deals only with information from the closed bands. Thus if a resonance appears in the diagonal  $K$ -matrix elements (the elastic scattering processes), it will appear at the same energy in the off-diagonal elements (in the inelastic scattering processes).

## V. LATTICE SCATTERING LENGTH

Just as in normal lattice-free scattering in one dimension, we can define the 1D lattice scattering length. In contrast, the

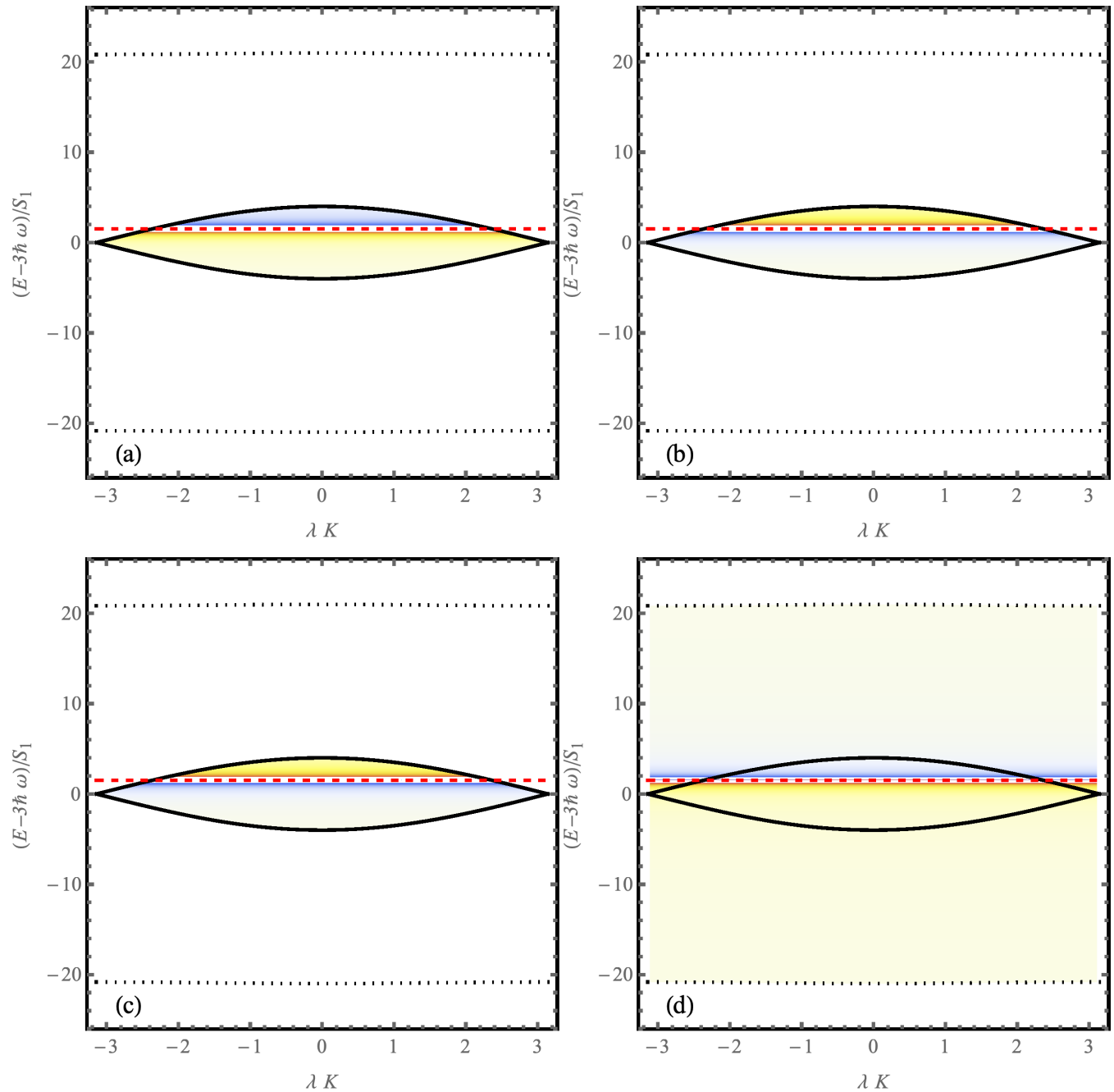


FIG. 2. The matrix elements of  $\bar{v}_g^{1/2} \mathbf{K}^L \bar{v}_g^{1/2}$  for scattering with harmonic oscillator Wannier states are shown as color density plots. Here we included the  $\{0, 0\}$ ,  $\{1, 1\}$ , and the symmetrized  $\{0, 2\}$  two-body bands, and are showing the  $K$  matrix for scattering in the overlapping excited states. (a) and (d) show the matrix elements for elastic scattering in the  $\{1, 1\}$  and  $\{0, 2\}$  states, respectively. (b) and (c) show the matrix elements for inelastic scattering  $\{1, 1\} \rightarrow \{0, 2\}$  and  $\{0, 2\} \rightarrow \{1, 1\}$ , respectively. The lattice and interaction parameters are the same as in Fig. 1(b). The yellow and blue regions represent positive and negative values of the  $K$ -matrix element, respectively, with the darker color representing a larger magnitude.

scattering length in the presence of a lattice can be defined as the relative quasimomentum reaches the edge of a two-body band either at the top or the bottom of the band, here when  $\lambda k \rightarrow 0, \pi$ :

$$\lim_{k \rightarrow 0} k \mathbf{K}_{\mu\nu \rightarrow \mu\nu}^L = \frac{1}{a_{\mu\nu}^{(-)}},$$

$$\lim_{k \rightarrow \pi/\lambda} \left( \frac{\pi}{\lambda} - k \right) \mathbf{K}_{\mu\nu \rightarrow \mu\nu}^L = \frac{1}{a_{\mu\nu}^{(+)}}. \quad (27)$$

Here  $a_{\mu\nu}^{(-)}$  and  $a_{\mu\nu}^{(+)}$  is the scattering length at the bottom and top of the two-body band, respectively, corresponding to elastic scattering in the  $\{\mu\nu\}$  band. In the two-band approximation from above this yields

$$\frac{\lambda J_K^{00}}{a_{00}^{(\pm)}} = - \left[ U_{00} - \frac{U_{01}^2}{U_{11} + \sqrt{(E_{00}^{(\pm)} - \varepsilon_{11})^2 - (2J_K^{11})^2}} \right], \quad (28)$$

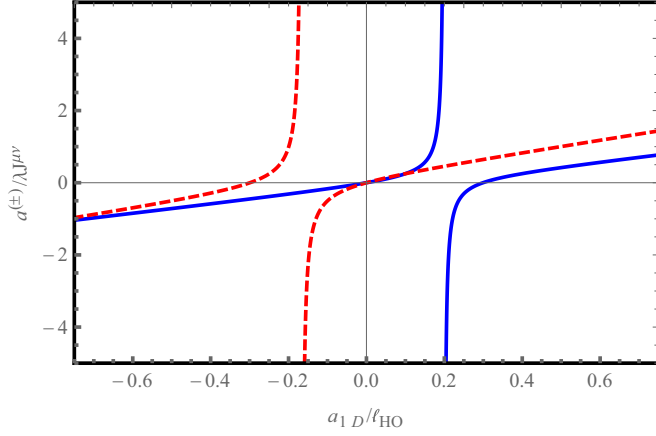


FIG. 3. The lattice scattering length  $a^{(\pm)}$  is shown in the  $\{0, 0\}$  (blue solid curve) and  $\{1, 1\}$  (red dashed curve) two-body bands is shown as a function of the 1D scattering length  $a_{1D}$  for a lattice with lattice spacing  $\lambda = 8\ell_{HO}$ . For a lattice this deep, the hopping energy is much smaller than the local oscillator energy and thus  $a^{(+)} \approx a^{(-)}$ .

$$\frac{\lambda J_K^{11}}{a_{11}^{(\pm)}} = - \left[ U_{11} - \frac{U_{01}^2}{U_{00} - \sqrt{(E_{11}^{(\pm)} - \varepsilon_{00})^2 - (2J_K^{00})^2}} \right]. \quad (29)$$

Here  $E_{\mu\nu}^{(\pm)} = \varepsilon_{\mu\nu} \pm 2J_K^{\mu\nu}$  is the energy at the top (+) and bottom (-) of the band.

Contrary to the 3D case, strong effective interactions occur in one dimension near zeros in the scattering length. Conversely, poles in the scattering length occur at zeros in the lattice  $K$  matrix near the top or bottom of the two-body bands. Figure 3 shows the lattice scattering length  $a_{\mu\nu}^{(\pm)}$  for the lowest and first excited two-body band within the two-band approximation plotted as a function of the free-space 1D scattering length  $a_{1D}$ . We again assumed that the lattice sites are deep enough to each be treated as local harmonic oscillators with lattice spacing  $\lambda = 8\ell_{HO}$ . We observe that at finite values of the 1D free-space scattering length, there are poles in the lattice scattering length corresponding to areas of weak effective interaction. The zeros in the lattice scattering length correspond to strong, resonant effective interactions. While we show the  $K = 0$  scattering lengths here, similar structures with small shifts appear for all values of the center-of-mass quasimomentum. In the case of a deep lattice such as that used here, the hopping energy becomes much smaller than the local oscillator energy, and thus much smaller than the band-gap energy. When the on-site interaction energy is much larger than the hopping energy for all center-of-mass quasimomenta ( $|U_{\mu\nu}^{\mu'\nu'}| \gg |J^{\mu\nu}|$ ) the quasimomentum dependence of the

lattice scattering length drops out from the right-hand side of Eqs. (28) and (29). In addition, when the hopping energy is small compared to the interaction energy, there is effectively no difference between  $a_{\mu\nu}^{(+)}$  and  $a_{\mu\nu}^{(-)}$ .

Large positive lattice scattering lengths correspond to a weakly bound state. Within the lattice approximations made here, the energy of the bound state is given approximately by

$$E_{bnd} \approx \varepsilon_{\mu\nu} \pm J_K^{\mu\nu} \sqrt{4 + \left( \frac{\lambda}{a_{\mu\nu}^{(\pm)}} \right)^2}, \quad (30)$$

with the approximation becoming exact at unitarity, i.e.,  $|a_{\mu\nu}^{(\pm)}| \rightarrow \infty$ . Note that poles in the lattice scattering length occur when that bound state becomes degenerate with the two-body band continuum.

## VI. SUMMARY

In this study we explored two-body scattering in the presence of a 1D lattice. By transforming into a basis of Wannier states and removing the discrete center-of-mass position we derived the multiband Green's operator including contributions from both energetically open and closed bands. This Green's operator was then used with in the Lippmann-Schwinger equation to extract the lattice  $K$  matrix.

In the case of on-site interactions, the  $K$  matrix consists of two terms, the first, which is proportional to the open-channel interaction matrix, correspond to scattering between the energetically open two-body bands, while the second term accounts for virtual scattering events into energetically closed bands allowing for resonant scattering. In the absence of coupling between closed band, resonances occur when bound states attached to closed bands are embedded in the open bands.

The expression for the scattering  $K$  matrix derived here incorporates the scattering contributions from any number of overlapping open bands with any number of closed bands. In deriving Eq. (23) we assumed nearest-neighbor hopping and on-site interactions only. However, as the band index increases, the contributions from distant hopping will become larger, and will not necessarily be negligible. Additionally, higher index Wannier states will become less and less localized to the point where individual states span multiple sites inducing beyond nearest-neighbor hopping and creating nearest-neighbor (or even longer-range) interactions. Higher-band contributions in 3D lattices were directly incorporated for scattering in the lowest band in the zero center-of-mass quasimomentum regime in Refs. [31,37]. Properly incorporating higher-energy bands in the  $K$  matrix as well as extending these results to higher dimensions is the focus of ongoing work.

## APPENDIX

Starting from the  $K$ -matrix element given in Eq. (22) we wish to show the result of Eq. (23) in the case of on-site interactions. Expanding the scattering states  $|f_{i(j)}\rangle$  and inserting a complete set of Wannier states yields

$$\mathbf{K}_{ji}^L = -2\pi \left[ \sum_{l \in \text{open}} \sum_{z, z'} f_j^+(z') \langle \mathbf{j}z' | \hat{D}^{-1} | \mathbf{l}z \rangle \langle \mathbf{l}z | \hat{U} | \mathbf{i}z \rangle f_i^+(z) + \sum_{l \in \text{closed}} \sum_{z, z'} f_j^+(z') \langle \mathbf{j}z' | \hat{D}^{-1} | \mathbf{l}z \rangle \langle \mathbf{l}z | \hat{U} | \mathbf{i}z \rangle f_i^+(z) \right], \quad (A1)$$



where  $\hat{D} = (\mathbb{1} + \hat{U}\hat{G})$  and we dropped the center-of-mass quasimomentum  $K$  dependence everywhere for notational simplicity. Note that we split the sum over the band indices into the contributions from the  $N$  open and  $M$  closed bands. We used the fact that  $\langle \mathbf{l}z'' | \hat{U} | \mathbf{l}z \rangle = \langle \mathbf{l}z | \hat{U} | \mathbf{l}z \rangle \delta_{zz''}$ . We now wish to invert  $\hat{D}$  in the basis of Wannier states which can be broken into four blocks:

$$\bar{D} = \begin{pmatrix} \bar{D}_{oo} & \bar{D}_{oc} \\ \bar{D}_{co} & \bar{D}_{cc} \end{pmatrix},$$

where  $\bar{D}$  is the operator  $\hat{D}$  expressed as a matrix in the Wannier basis whose the matrix elements are given by

$$\begin{aligned} \bar{D}_{\mathbf{j}\mathbf{l}}(z', z) &= \langle \mathbf{j}z' | \hat{D} | \mathbf{l}z \rangle \\ &= \delta_{\mathbf{j}\mathbf{l}} \delta_{z'z} + e^{i(\phi_{\mathbf{k}}^{\mathbf{l}} - \phi_{\mathbf{k}}^{\mathbf{j}})z'} U_{\mathbf{j}\mathbf{l}}(|z'|) g_{\mathbf{l}}(z, z'). \end{aligned}$$

Here  $\bar{D}_{oo}(z, z')$  is an  $N \times N$  matrix where both  $\mathbf{j}$  and  $\mathbf{l}$  correspond to open bands,  $\bar{D}_{co}(z, z')$  is an  $M \times N$  matrix where  $\mathbf{j}$  is a closed band and  $\mathbf{l}$  is open,  $\bar{D}_{oc}(z, z')$  is an  $N \times M$  matrix where  $\mathbf{j}$  is an open band and  $\mathbf{l}$  is closed, and  $\bar{D}_{cc}(z, z')$  is an  $M \times M$  matrix where both  $\mathbf{j}$  and  $\mathbf{l}$  correspond to closed bands. Notice that the only difference between the closed and open bands is the LGF  $g_{\mathbf{l}}(z, z')$  used. Thus the form of the matrix elements for  $\bar{D}_{oo}(z, z')$  and  $\bar{D}_{co}(z, z')$  are the same given by

$$\bar{D}_{\mathbf{j}\mathbf{l}}(z', z) = \delta_{\mathbf{j}\mathbf{l}} \delta_{z'z} + 2\pi e^{i(\phi_{\mathbf{k}}^{\mathbf{l}} - \phi_{\mathbf{k}}^{\mathbf{j}})z'} U_{\mathbf{j}\mathbf{l}}(|z'|) f_{\mathbf{l}}^+(z_{>}) f_{\mathbf{l}}^-(z_{<}). \quad (\text{A2})$$

Similarly, the form of the matrix elements for  $\bar{D}_{cc}(z, z')$  and  $\bar{D}_{oc}(z, z')$  are of the same given by

$$\bar{D}_{\mathbf{j}\mathbf{l}}(z', z) = \delta_{\mathbf{j}\mathbf{l}} \delta_{z'z} + e^{i(\phi_{\mathbf{k}}^{\mathbf{l}} - \phi_{\mathbf{k}}^{\mathbf{j}})z'} U_{\mathbf{j}\mathbf{l}}(|z'|) \frac{\alpha_1^{|z-z'|+1}}{J_K^{\mu\nu} (1 - \alpha_1^2)}, \quad (\text{A3})$$

where  $\alpha_1$  is given by Eq. (18).

Inverting  $\bar{D}$  directly gives

$$\bar{D}^{-1} = \begin{pmatrix} (\bar{D}_{oo} - \bar{D}_{oc} \bar{D}_{cc}^{-1} \bar{D}_{co})^{-1} & -\bar{D}_{cc}^{-1} \bar{D}_{co} (\bar{D}_{oo} - \bar{D}_{oc} \bar{D}_{cc}^{-1} \bar{D}_{co})^{-1} \\ -\bar{D}_{oo}^{-1} \bar{D}_{oc} (\bar{D}_{cc} - \bar{D}_{co} \bar{D}_{oo}^{-1} \bar{D}_{oc})^{-1} & (\bar{D}_{cc} - \bar{D}_{co} \bar{D}_{oo}^{-1} \bar{D}_{oc})^{-1} \end{pmatrix}.$$

In Eq. (A1), we are only concerned with the open-open segment. Inserting  $\bar{D}$  and carrying out the matrix multiplication gives

$$\mathbf{K}_{\mathbf{j}\mathbf{l}}^L = -2\pi \left\{ \sum_{z, z'} f_{\mathbf{j}}^+(z') [(\bar{D}_{oo} - \bar{D}_{oc} \bar{D}_{cc}^{-1} \bar{D}_{co})^{-1} \bar{U}_{oo}]_{\mathbf{j}\mathbf{l}} f_{\mathbf{l}}^+(z) - \sum_{z, z'} f_{\mathbf{j}}^+(z') [\bar{D}_{oo}^{-1} \bar{D}_{oc} (\bar{D}_{cc} - \bar{D}_{co} \bar{D}_{oo}^{-1} \bar{D}_{oc})^{-1} \bar{U}_{co}]_{\mathbf{j}\mathbf{l}} f_{\mathbf{l}}^+(z) \right\}, \quad (\text{A4})$$

where  $\bar{U}_{\mathbf{j}\mathbf{l}} = e^{i(\phi_{\mathbf{k}}^{\mathbf{l}} - \phi_{\mathbf{k}}^{\mathbf{j}})z} U_{\mathbf{j}\mathbf{l}}(|z|)$  are matrix elements of the interaction in the two-body Wannier basis.

Equation (A4) is general for interactions of any range. Here, we are concerned with on-site interactions where  $\bar{U}_{\mathbf{j}\mathbf{l}} = e^{i(\phi_{\mathbf{k}}^{\mathbf{l}} - \phi_{\mathbf{k}}^{\mathbf{j}})z} U_{\mathbf{j}\mathbf{l}} \delta_{z,0}$ . Inserting this collapses the double sum and we may evaluate this at  $z = z' = 0$ . We may also note that  $f_{\mathbf{l}}^-(0) = 0$  while  $f_{\mathbf{l}}^+(0) = \sqrt{\lambda/\pi} v_g^{\mathbf{l}}$ . This simplifies the expression for the  $D_{\mathbf{j}\mathbf{l}}$  matrix elements considerably for open channels leaving  $\bar{D}_{oo} = \mathbb{1}$  and  $\bar{D}_{co} = 0$ . Inserting this gives

$$\begin{aligned} \mathbf{K}_{\mathbf{j}\mathbf{l}}^L &= -2\pi \left\{ \sum_{z, z'} f_{\mathbf{j}}^+(z') [\bar{U}_{oo}]_{\mathbf{j}\mathbf{l}} f_{\mathbf{l}}^+(z) - \sum_{z, z'} f_{\mathbf{j}}^+(z') [\bar{D}_{oc} \bar{D}_{cc}^{-1} \bar{U}_{co}]_{\mathbf{j}\mathbf{l}} f_{\mathbf{l}}^+(z) \right\}, \\ &= -2\lambda (v_g^{\mathbf{l}} v_g^{\mathbf{j}})^{-1/2} [\mathcal{U}_{oo} - \mathcal{U}_{oc} \bar{g}_c (\mathbb{1} + \mathcal{U}_{cc} \bar{g}_c)^{-1} \mathcal{U}_{co}]_{\mathbf{j}\mathbf{l}}, \end{aligned}$$

which is the expression that appears in Eq. (23).

[1] I. Bloch, *Nat. Phys.* **1**, 23 (2005).

[2] I. Bloch, J. Dalibard, and W. Zwerger, *Rev. Mod. Phys.* **80**, 885 (2008).

[3] K. Günter, T. Stöferle, H. Moritz, M. Köhl, and T. Esslinger, *Phys. Rev. Lett.* **96**, 180402 (2006).

[4] M. Lewenstein, L. Santos, M. A. Baranov, and H. Fehrmann, *Phys. Rev. Lett.* **92**, 050401 (2004).

[5] C. Chin, R. Grimm, P. Julienne, and E. Tiesinga, *Rev. Mod. Phys.* **82**, 1225 (2010).

[6] M. Greiner, O. Mandel, T. Esslinger, T. W. Hänsch, and I. Bloch, *Nature* **415**, 39 (2002).

[7] M. P. A. Fisher, P. B. Weichman, G. Grinstein, and D. S. Fisher, *Phys. Rev. B* **40**, 546 (1989).

[8] W. S. Bakr, A. Peng, M. E. Tai, R. Ma, J. Simon, J. I. Gillen, S. Foelling, L. Pollet, and M. Greiner, *Science* **329**, 547 (2010).

[9] J. F. Sherson, C. Weitenberg, M. Endres, M. Cheneau, I. Bloch, and S. Kuhr, *Nature* **467**, 68 (2010).

- [10] D. Greif, M. F. Parsons, A. Mazurenko, C. S. Chiu, S. Blatt, F. Huber, G. Ji, and M. Greiner, *Science* **351**, 953 (2016).
- [11] L. W. Cheuk, M. A. Nichols, K. R. Lawrence, M. Okan, H. Zhang, and M. W. Zwierlein, *Phys. Rev. Lett.* **116**, 235301 (2016).
- [12] A. K. Fedorov, V. I. Yudson, and G. V. Shlyapnikov, *Phys. Rev. A* **95**, 043615 (2017).
- [13] S. Autti, P. J. Heikkinen, J. T. Mäkinen, G. E. Volovik, V. V. Zavjalov, and V. B. Eltsov, *Nat. Mater.* **20**, 171 (2021).
- [14] S. Choi, J. Choi, R. Landig, G. Kucsko, H. Zhou, J. Isoya, F. Jelezko, S. Onoda, H. Sumiya, V. Khemani *et al.*, *Nature* **543**, 221 (2017).
- [15] J. Zhang, P. W. Hess, A. Kyprianidis, P. Becker, A. Lee, J. Smith, G. Pagano, I.-D. Potirniche, A. C. Potter, A. Vishwanath *et al.*, *Nature* **543**, 217 (2017).
- [16] F. Wilczek, *Phys. Rev. Lett.* **109**, 160401 (2012).
- [17] K. Sacha and J. Zakrzewski, *Rep. Prog. Phys.* **81**, 016401 (2017).
- [18] K. Sacha, *Phys. Rev. A* **91**, 033617 (2015).
- [19] A. Lazarides, A. Das, and R. Moessner, *Phys. Rev. Lett.* **112**, 150401 (2014).
- [20] A. Lazarides, A. Das, and R. Moessner, *Phys. Rev. Lett.* **115**, 030402 (2015).
- [21] S. Mistakidis, L. Cao, and P. Schmelcher, *J. Phys. B: At., Mol. Opt. Phys.* **47**, 225303 (2014).
- [22] S. I. Mistakidis, L. Cao, and P. Schmelcher, *Phys. Rev. A* **91**, 033611 (2015).
- [23] T. Plaßmann, S. I. Mistakidis, and P. Schmelcher, *J. Phys. B: At., Mol. Opt. Phys.* **51**, 225001 (2018).
- [24] P. Siegl, S. I. Mistakidis, and P. Schmelcher, *Phys. Rev. A* **97**, 053626 (2018).
- [25] K. Winkler, G. Thalhammer, F. Lang, R. Grimm, J. Hecker Denschlag, A. J. Daley, A. Kantian, H. P. Büchler, and P. Zoller, *Nature* **441**, 853 (2006).
- [26] M. Valiente and D. Petrosyan, *J. Phys. B: At., Mol. Opt. Phys.* **41**, 161002 (2008).
- [27] N. Nygaard, R. Piil, and K. Mølmer, *Phys. Rev. A* **78**, 023617 (2008).
- [28] D. Petrosyan, B. Schmidt, J. R. Anglin, and M. Fleischhauer, *Phys. Rev. A* **76**, 033606 (2007).
- [29] R. Piil and K. Mølmer, *Phys. Rev. A* **76**, 023607 (2007).
- [30] M. Grupp, R. Walser, W. P. Schleich, A. Muramatsu, and M. Weitz, *J. Phys. B: At., Mol. Opt. Phys.* **40**, 2703 (2007).
- [31] P. O. Fedichev, M. J. Bijlsma, and P. Zoller, *Phys. Rev. Lett.* **92**, 080401 (2004).
- [32] J. von Stecher, V. Gurarie, L. Radzihovsky, and A. M. Rey, *Phys. Rev. Lett.* **106**, 235301 (2011).
- [33] M. Wouters and G. Orso, *Phys. Rev. A* **73**, 012707 (2006).
- [34] D. B. M. Dickerscheid, U. Al Khawaja, D. van Oosten, and H. T. C. Stoof, *Phys. Rev. A* **71**, 043604 (2005).
- [35] H. Terrier, J.-M. Launay, and A. Simoni, *Phys. Rev. A* **93**, 032703 (2016).
- [36] M. Valiente, *Phys. Rev. A* **81**, 042102 (2010).
- [37] X. Cui, Y. Wang, and F. Zhou, *Phys. Rev. Lett.* **104**, 153201 (2010).
- [38] T. Bergeman, M. G. Moore, and M. Olshanii, *Phys. Rev. Lett.* **91**, 163201 (2003).
- [39] D. C. Mattis, *Rev. Mod. Phys.* **58**, 361 (1986).
- [40] M. Valiente, D. Petrosyan, and A. Saenz, *Phys. Rev. A* **81**, 011601(R) (2010).
- [41] S. Paul, P. R. Johnson, and E. Tiesinga, *Phys. Rev. A* **93**, 043616 (2016).
- [42] G. Orso and G. V. Shlyapnikov, *Phys. Rev. Lett.* **95**, 260402 (2005).
- [43] P. O. Fedichev, M. W. Reynolds, and G. V. Shlyapnikov, *Phys. Rev. Lett.* **77**, 2921 (1996).
- [44] M. Aymar, C. H. Greene, and E. Luc-Koenig, *Rev. Mod. Phys.* **68**, 1015 (1996).